

Seasonal characteristics of water-soluble inorganic ions and carbonaceous aerosols in total suspended particulate matter at a rural semi-arid site, Kadapa (India)

G. Reshma Begam¹ · C. Viswanatha Vachaspati¹ · Y. Nazeer Ahammed¹ · K. Raghavendra Kumar² · R. R. Reddy³ · S. K. Sharma⁴ · Mohit Saxena⁴ · T. K. Mandal⁴

Received: 18 May 2016 / Accepted: 16 October 2016 / Published online: 29 October 2016
© Springer-Verlag Berlin Heidelberg 2016

Abstract To better understand the sources as well as characterization of regional aerosols at a rural semi-arid region Kadapa (India), size-resolved composition of atmospheric particulate matter (PM) mass concentrations was sampled and analysed. This was carried out by using the Anderson low-pressure impactor for a period of 2 years during March 2013–February 2015. Also, the variations of organic carbon (OC), elemental carbon (EC) and water-soluble inorganic ion components (WSICs) present in total suspended particulate matter (TSPM) were studied over the measurement site. From the statistical analysis, the PM mass concentration showed a higher abundance of coarse mode particles than the fine mode during pre-monsoon season. In contrast, fine mode

particles in the PM concentration showed dominance over coarse mode particle contribution during the winter. During the post-monsoon season, the percentage contributions of coarse and fine fractions were equal, whereas during the monsoon, coarse mode fraction was approximately 26 % higher than the fine mode. This distinct feature in the case of fine mode particles during the studied period is mainly attributed to large-scale anthropogenic activities and regional prevailing meteorological conditions. Further, the potential sources of PM have been identified qualitatively by using the ratios of certain ions. A high sulphate (SO₄) concentration at the measurement site was observed during the studied period which is caused by the nearby/surrounding mining activity. Carbon fractions (OC and EC) were also analysed from the TSPM, and the results indicated (OC/EC ratio of ~4.2) the formation of a secondary organic aerosol. At last, the cluster backward trajectory analyses were also performed at Kadapa for different seasons to reveal the origin of sources from long-range transport during the study period.

Responsible editor: Gerhard Lammel

Electronic supplementary material The online version of this article (doi:10.1007/s11356-016-7917-1) contains supplementary material, which is available to authorized users.

✉ Y. Nazeer Ahammed
ynahammed@gmail.com

¹ Atmospheric Science Laboratory, Department of Physics, Yogi Vemana University, Kadapa, Andhra Pradesh 516 003, India

² Collaborative Innovation Centre for Forecast and Evaluation of Meteorological Disasters, Key Laboratory for Aerosol-Cloud-Precipitation of China Meteorological Administration, School of Atmospheric Physics, Nanjing University of Information Science and Technology, Nanjing, Jiangsu 210044, China

³ Aerosol and Atmospheric Research Laboratory, Department of Physics, Sri Krishnadevaraya University, Anantapur, Andhra Pradesh 515 003, India

⁴ CSIR-National Physical Laboratory, DR. K S Krishna Road, New Delhi 110 012, India

Keywords Total suspended particulate matter · WSIC · Carbonaceous aerosols · HYSPLIT · Semi-arid

Introduction

Particulate matter (PM) is an important component of pollutant which can be widely variable according to the formation, size, source, composition and geographical location (Rodriguez et al. 2007a). PM is particularly suitable to define the air pollution level in an area and its associated environmental and health impacts (WHO 2005). In general, PM can be addressed as solid and liquid particles that are injected into the atmosphere by natural and anthropogenic activities.

Depending on the different formation mechanism process, PM can be classified as primary (Navrátil et al. 2013) and secondary particles (Cheung et al. 2013).

Generally, particles with diameter $>2.5 \mu\text{m}$ can be defined as coarse mode; similarly, particles having diameters $<2.5 \mu\text{m}$ and $<100 \text{ nm}$ are defined as fine mode and ultrafine particles, respectively. Whereas, the particles with a diameter not more than 40 to 50 μm are mentioned as total suspended particulate matter (TSPM) (Seinfeld and Pandis 1998). The composition and size distribution of PM and their associated impacts on health and environment (global as well as regional) depend strongly on particle formation processes, i.e., the sources of the particles. This has been explored by several researchers in numerous studies as PM_{10} , $\text{PM}_{2.5}$ and PM_{10} (Pillai and Moorthy 2001; Gerasopoulos et al. 2007; Balakrishnaiah et al. 2011; Contini et al. 2014).

Water-soluble inorganic ion components (WSICs) are major components of fine particles and account for about 50 % of $\text{PM}_{2.5}$ (Cao et al. 2003; Xiang et al. 2017). WSIC can affect the size, composition, number density, acidity and lifetime of aerosols due to their strong hygroscopic property (Cao et al. 2003). Carbonaceous aerosols are another important fraction in the atmosphere. They have a significant effect on global climate change through direct and indirect radiative forcing. Based on thermal and optical properties, carbonaceous aerosols can be divided into organic carbon (OC) and elemental carbon (EC). OC is an important parameter responsible for the increase of cloud albedo, which, in turn, alters global climate change (Dan et al. 2004). OC is emitted by fossil fuel combustion or formed by a complex process of secondary formation (Cao et al. 2003), whereas EC can be emitted directly by incomplete combustion of biomass and fossil fuel. EC in the atmosphere also plays a significant role in global warming (O'Brien and Mitchel 2003; Dan et al. 2004), which, in turn, reduces visibility (Na et al. 2004) through absorption and scattering of solar radiation (Ramanathan et al. 2001).

The present study gives good insight into the detailed measurements and analysis of size-segregated mass concentration of PM at a semi-arid rural site over Kadapa situated in the southern part of India for a period of 2 years (March 2013 to February 2015). To the best of our knowledge from the literature review, these are the first long-term measurements to estimate the PM mass concentrations (monthly and seasonal) over the Indian subcontinent. The observations were carried out over a semi-arid region for which there existed a gap in terms of aerosol mass concentration and size distribution. Apart from this, we also derived the information on the WSIC (70 samples) and carbonaceous aerosols (OC and EC of 80 samples) from the TSPM samples, in order to understand the chemical characteristics of regional atmospheric aerosols. The structure of the paper is organized as follows. The details of the observational site and prevailing local meteorology are illustrated in the “[Sampling site and](#)

[meteorology](#)” section; followed by the instrumentation and methodology are described in the “[Instrument and methods](#)” section. The “[Results and discussion](#)” section demonstrates the monthly and seasonal variations of PM and associated WSIC and carbonaceous fractions in the PM. Finally, the main conclusions drawn from this study are provided in the “[Conclusions](#)” section.

Sampling site and meteorology

Kadapa is a tropical semi-arid station located in the southern part of India (see Fig. 1) in the state of Andhra Pradesh. It is an active station under Aerosol Radiative Forcing over India (ARFI) network of stations. The TSPM samples were collected on the roof of the Science Block Building within the vicinity of the Yogi Vemana University (YVU; 14.47° N , 78.81° E , 138 m above mean sea level) campus, Kadapa. The observational site (YVU) is situated adjacent to the highway and is about 15 km west of the main city of Kadapa, where automobile and vehicular emissions are the principle sources of air pollution. In addition, there are several brick kilns and some small-scale cement and electrical industries around the observational site situated within 30-km radius. Further, there are a lot of both opencast and underground mining activities taking place at the Kadapa Basin (Begam et al. 2016) and may have a significant impact due to higher PM mass concentration. These act as a source for various types of aerosol particles in the area and deserve to be studied more in the future.

Ambient TSPM samples were collected for a period of 2 years during March 2013–February 2015 spread over all the major seasons: winter (December–January–February (DJF)), pre-monsoon/summer (March–April–May (MAM)), monsoon (June–July–August (JJA)) and post-monsoon (September–October–November (SON)). Surface level ambient air temperature, relative humidity, rainfall, wind speed and wind direction data were recorded from the portable automatic weather station, installed on the roof of the building in the YVU campus, Kadapa. Figure 2 shows the variations of meteorological parameters observed over the site during the studied period. The meteorology that prevails over Kadapa is generally hot and humid. The daily temperature values can rise up to ($\sim 43^\circ \text{ C}$) during pre-monsoon season. Monthly temperature was started to increase from December/January onwards and attains its peak in April ($32.6 \pm 0.14^\circ \text{ C}$) and May ($33.1 \pm 0.14^\circ \text{ C}$) and then gradually decreased during monsoon and winter seasons (Fig. 2a). Seasonally, high and low temperatures were recorded during pre-monsoon (32° C) and winter seasons (24° C), respectively. Whereas, the low and high mean values of relative humidity were observed during pre-monsoon (43 %) and post-monsoon (68 %) seasons, which were in the range from 15 to 80 % and 25 to 100 %, respectively, during the studied period.



Fig. 1 Terrain map of Peninsular India (*top left side panel*) showing the location of measurement site Kadapa (*black solid circle*) along with other stations under ARFI network. Also shown is the location of the Yogi

Vemana University (YVU) campus area in Kadapa (*top right side panel*) and the satellite aerial view of the sampling site building in the YVU campus indicated with a *yellow colour arrow* (*black hollow circle*)

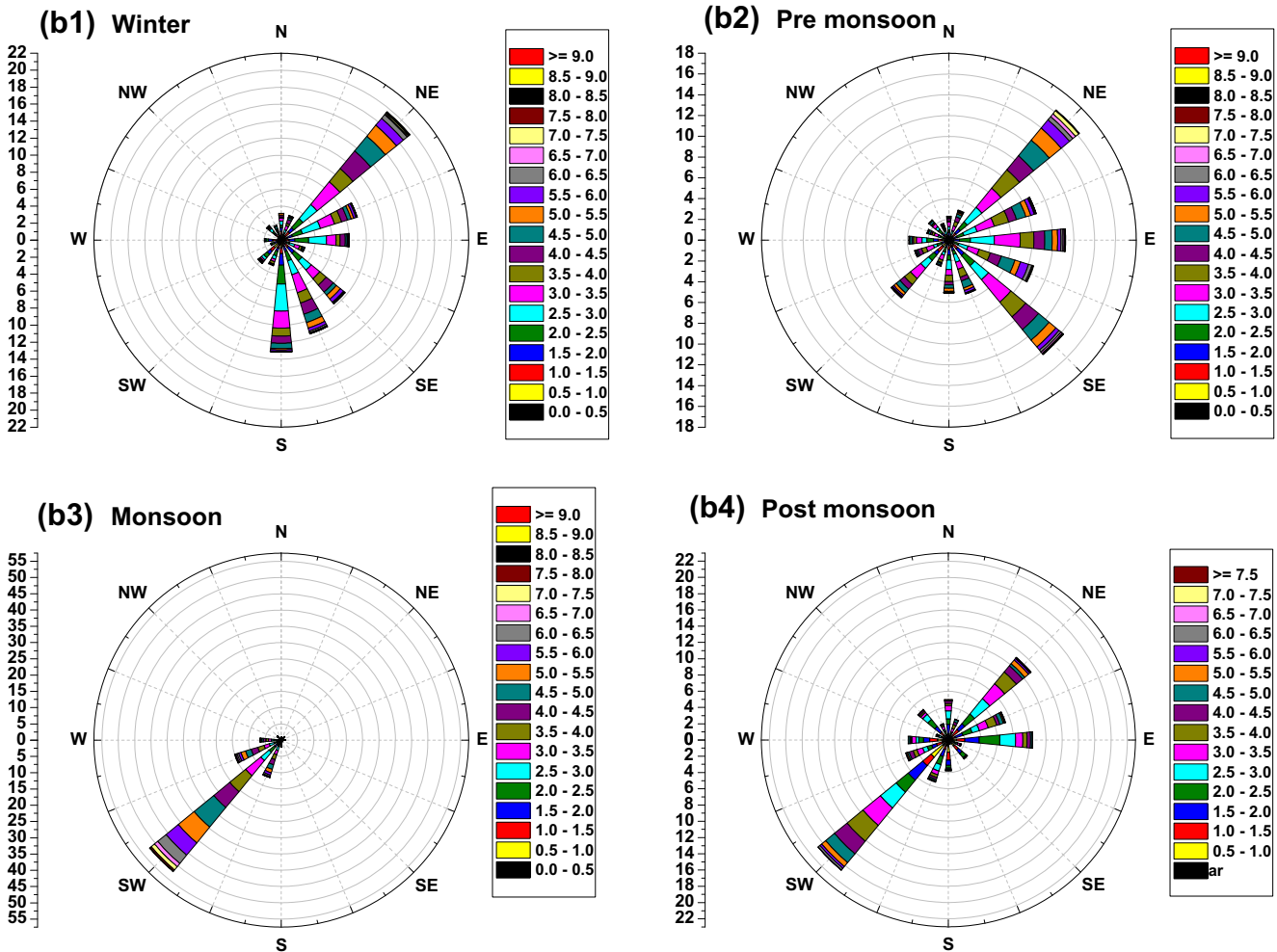
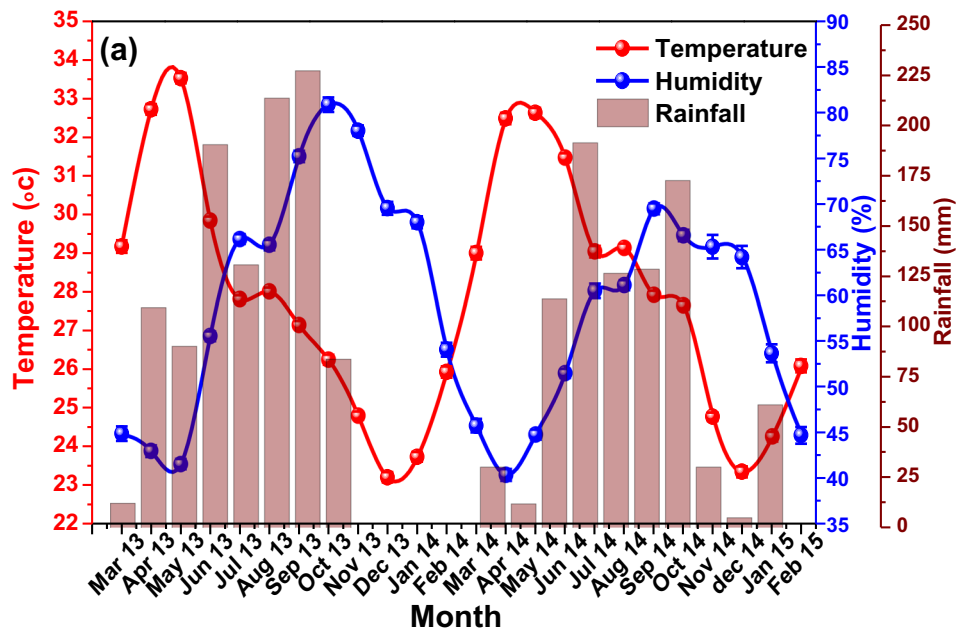
Kadapa received comparatively very low annual rainfall from both the southwest and northeast monsoons, which was about 529 mm against the total annual rainfall of 800 mm in a year over India (Begam et al. 2016). The highest rainfall was observed during the post-monsoon (143 mm) and monsoon (141 mm) seasons, with the higher relative humidity levels that exist over the measurement site (Fig. 2a). High wind speeds ($>9 \text{ m s}^{-1}$) were observed during the monsoon blowing from southwest direction bringing pristine marine air masses (see Fig. 2b). Then, the winds are shifted to northeast direction with moderate winds experienced during the post-

monsoon ($6\text{--}9 \text{ m s}^{-1}$) and winter ($7\text{--}9 \text{ m s}^{-1}$) seasons. Further, the winds became stronger during the pre-monsoon season ranging from 8 to 9 m s^{-1} .

Instrument and methods

Measurements

Different size fractions of PM have been collected by using a cascade impactor sampler with eight stages (TE 20–800,



Thermo Fischer Scientific Air Quality Instruments, USA). The instrument sucks the ambient air at a constant flow rate

of 28.3 l min⁻¹ (<http://www.newstarencvironmental.com>). Flow rate of the sampler checked regularly to maintain

Fig. 2 a Monthly variations of meteorological parameters such as temperature, relative humidity and rainfall. **b** Wind rose plots showing wind direction observed at the Kadapa for all the seasons along with the wind speed during the study period. The wind speed is indicated with the colour scale shown adjacent to panels. Each *circle* represents percentage of occurrences (2 % each for all the seasons, except for the monsoon with 5 %)

constant air flow during the sampling. PM samples were collected on a Whatman quartz microfibre (81 mm) filter paper, and each sampling was carried out continuously for a time period of 72 h (3 days). If any power failure was noticed during the sampling time, then sampling hours were extended to reach the target time. The sampling was performed at a rate of $1.68 \text{ m}^3 \text{ h}^{-1}$ and in total $40.32 \text{ m}^3 \text{ day}^{-1}$ of air passed through each filter. The cascade impactor separates the ambient air particles into eight size fractions (0–10.0 μm) depending on the equivalent aerodynamic cut-off diameter: 10.0–9.0 μm (stage 0), 9.0–5.8 μm (stage 1), 5.8–4.7 μm (stage 2), 4.7–3.3 μm (stage 3), 3.3–2.1 μm (stage 4), 2.1–1.1 μm (stage 5), 1.1–0.7 μm (stage 6), 0.7–0.4 μm (stage 7) and 0.4–0 μm (stage 8). More information regarding the operation and the set-up of the instrument can be found in Singh et al. (2013).

Two sets of size-segregated PM samples were collected in a month during the weekdays from Tuesday to Thursday (following the standard protocol given under the ARFI network of stations) for the whole measurement period. The sampling observations were a lack in the month of October 2013 due to malfunction or technical problems of the instrument at the measurement site. After the collection of samples, the samples were kept in electronic desiccators for conditioning. High volume air sampler (HV-1E, F&J Specialty Products, Inc. (<http://www.fjspecialty.com>)) was also used to collect ambient air TSPM samples on 47-mm diameter quartz fibre filters during the study period. The TSPM samples were collected regularly twice in a week, i.e., only on Wednesday with one in the morning from 5:00 local time (LT, UTC + 5:30 h) to 9:00 LT and other in the evening from 18:00 LT to 22:00 LT.

Chemical analysis

The quartz fibre filter, which was used for the extraction of ions (cations and anions), was kept in a glass tube filled with 9 ml of deionized water at room temperature. After 40 min, the various WSIC ions (cations: Na^+ , NH_4^+ , K^+ , Mg^{2+} , Ca^{2+} ; anions: F^- , Cl^- , NO_3^- , NO_2^- , PO_4^{2-} and SO_4^{2-}) were recognized by the ion chromatography (DIONEX-ICS-3000, USA) from the extracted solution. The relative standard deviation of each ion was <6 % in reproducibility tests. Blank values were subtracted from sample determinations. More information about the analysis for the extraction of WSIC from TSPM samples is given elsewhere (Sharma et al. 2012b; Xiang et al. 2017). Further, all the samples were analysed for OC and EC by using a DRI Model 2001A Thermal/Optical

Carbon Analyser (Atmoslytic Inc., Calabasas, CA, USA). The temperature steps of the Interagency Monitoring of Protected Visual Environments (IMPROVE) thermal evolution protocol was adopted (Chow et al. 2001). A 0.5 cm^2 punch aliquot of each sample was heated stepwise at four temperature plateaus of 140 $^\circ\text{C}$ (OC1), 280 $^\circ\text{C}$ (OC2), 480 $^\circ\text{C}$ (OC3) and 580 $^\circ\text{C}$ (OC4) in a non-oxidizing helium atmosphere and at three temperatures of 580 $^\circ\text{C}$ (EC1), 740 $^\circ\text{C}$ (EC2) and 840 $^\circ\text{C}$ (EC3) in an oxidizing atmosphere of 2 % oxygen and 98 % helium atmosphere. This produced four OC fractions (OC1, OC2, OC3 and OC4), a pyrolysed carbon fraction (OP determined when reflected laser light attained its original intensity after oxygen was added to the combustion atmosphere) and three EC fractions (EC1, EC2 and EC3). Thus, the OC under IMPROVE protocol is operationally defined as OC1 + OC2 + OC3 + OC4 + OP and EC as EC1 + EC2 + EC3-OP.

Gravimetric analysis

In the present study, the TSPM samples, as well as PM mass concentrations derived for different size bins, were estimated by using the gravimetric technique. To dry up the samples, they were placed in the vacuum desiccators for ~24 h and then weighed by using analytical balance (Schimadzu Semi-Micro Dual Range Balance, Model AUW220D with a reading precision of 0.01 mg) before and after the sampling. More caution should be taken while measuring the mass concentration, in such a way that the effect of temperature (Temp) and RH on the weight should be nullified. Hence, first, the samples were conditioned for ~24 h at 20 $^\circ\text{C}$ and 40 % RH (Deshmukh et al. 2013; Satsangi et al. 2011) before and after the sampling to minimize the uncertainty in the estimation of mass concentration following the European standard method. Then, the mass concentrations were corrected for the blank values as suggested by several authors (e.g., Hieu and Lee 2010; Kopanakis et al. 2012; Deshmukh et al. 2013; Singh et al. 2013).

Results and discussion

Size distribution of PM

The regional aerosol size distribution mainly influenced by the sources of aerosols and/or emission processes (Gerasopoulos et al. 2007), which is highly variable with time depending on several factors like source strength and/or regional meteorology (Rodriguez et al. 2007b). The respective mean concentrations of PM_{10} , $\text{PM}_{2.5}$, $\text{PM}_{10-2.5}$ and PM_1 over the measurement site during the studied period were observed to be 61.4 ± 3.4 , 29.0 ± 3.5 , 32.4 ± 2.28 and $21.0 \pm 2.3 \mu\text{g m}^{-3}$. Similar variations of results with high mass concentrations for PM_{10} ,

PM_{2.5} and PM_{10–2.5} were also noticed by Pateraki et al. (2010) with 34.8, 18.0 and 23.8 $\mu\text{g m}^{-3}$ and Almeida et al. (2006) for PM_{2.5} and PM_{10–2.5} in the range 3.5–68 and 3.6–71 $\mu\text{g m}^{-3}$ over a suburban regions of Athens (Greece) and Lisbon (Portugal), respectively.

The season-wise percentage contributions of fine mode mass concentration in the PM₁₀ were 43, 37, 50 and 57 % in pre-monsoon, monsoon, post-monsoon and winter seasons, respectively. Similarly, the percentage contributions of coarse mode mass concentration in the PM₁₀ for the above respective seasons were around 57, 63, 50 and 43 %. During the pre-monsoon, coarse mode particles were higher than that of fine mode particles by 14 % and a contrasting feature has been noticed during winter with the same proportion. Whereas, the concentration proportions of both fine and coarse modes were equal in contribution to the TSPM concentration in post-monsoon season. But, the coarse mode concentration is higher than that of the fine mode by 26 % during the monsoon season. From the contour map of coarse mode particle (PM_{10–2.5}) concentration (see Fig. 5b), it is clear that the coarse mode particle concentration has consistently attained maximum when the winds are coming from the southwest direction which means the contribution of marine aerosols to the PM. Further, the local mineral dust as well as regional dust from the cement and brick industries may also influence the coarse mode particle concentration during the monsoon season. The same feature was revealed from the HYSPLIT trajectory analysis which will be discussed in the “Role of air mass transport pathways” section. The detailed statistical seasonal analysis of different size fractions of TSPM are tabulated in Table 1.

The seasonal variations of PM mass concentrations obtained from nine size regimes during the study period are shown in Fig. 4. The same has been derived on a monthly basis is presented in the Supplementary Material (SM) (see Fig. S2 of SM). The coarse mode particles mainly consist of airborne (windblown) particles produced from the deserts, salt particles from sea spray and mechanically generated mineral dust particles. In the present study for the bin size 4.7–5.8 μm , we noticed a peak in the coarse mode for all the seasons except during monsoon 2013, where the peak was shifted for the bin size 2.1–3.3 μm . In the case of fine mode, the peak appeared at the stage 0.7–1.1 μm in all the seasons except monsoon 2013, where the peak was shifted to the stage 0.4–0.7 μm (see Fig. 3). It is also evident that a bimodal aerosol size distribution with primary (coarse mode) and secondary (fine mode) peaks occurring at bin size 4.7–5.8 and 0.7–1.1 μm , respectively, at the measurement site except for the season monsoon 2013. The observed size distributions during the study period can be attributed to the regional anthropogenic activities which represent the seasonal characteristics of source particles. A similar bimodal distribution was observed by

Table 1 Seasonal variations of TSPM, PM mass fractions and their ratios along with OC and EC mass concentrations in TSPM during the study period observed at Kadapa

Season	TSPM ($\mu\text{g m}^{-3}$)	PM ₁₀ ($\mu\text{g m}^{-3}$)	PM _{2.5} ($\mu\text{g m}^{-3}$)	PM _{10–2.5} ($\mu\text{g m}^{-3}$)	BC fraction in TSPM	BC fraction in PM _{2.5}	PM _{2.5} /PM ₁₀	PM ₁₀ /PM _{2.5}	PM ₁₀ /PM ₁₀	OC ($\mu\text{g m}^{-3}$)	EC ($\mu\text{g m}^{-3}$)
Pre-monsoon 2013	93.9 ± 0.1	70.1 ± 2.7	30.8 ± 3.6	20.3 ± 2.6	39.3 ± 6.1	3.5	0.45	0.66	0.29	5.9 ± 0.1	1.6 ± 0.1
Monsoon 2013	64.9 ± 10.4	56.5 ± 11.3	21.7 ± 4.8	12.5 ± 2.9	34.8 ± 6.5	1.6	0.38	0.58	0.22	4.3 ± 0.4	0.6 ± 0.2
Post-monsoon 2013	70.0 ± 14.8	65.2 ± 3.0	31.6 ± 4.4	19.5 ± 2.3	33.6 ± 1.4	4.0	0.48	0.62	0.30	5.5 ± 2.2	2.1 ± 1.1
Winter 2014	72.6 ± 8.3	58.3 ± 1.0	33.1 ± 0.1	21.1 ± 0.9	25.2 ± 1.1	4.4	0.57	0.64	0.36	5.8 ± 1.0	2.5 ± 0.2
Pre-monsoon 2014	83.3 ± 9.7	59.5 ± 7.8	24.7 ± 3.2	17.0 ± 1.0	34.8 ± 4.6	3.0	0.42	0.69	0.28	6.3 ± 0.9	2.4 ± 0.6
Monsoon 2014	49.9 ± 4.7	48.1 ± 2.1	17.5 ± 1.9	10.1 ± 1.7	30.6 ± 0.3	2.2	0.36	0.58	0.21	3.9 ± 0.1	1.2 ± 0.3
Post-monsoon 2014	92.1 ± 34.7	71.4 ± 9.6	37.2 ± 8.5	23.1 ± 3.3	34.1 ± 3.4	1.5	0.51	0.62	0.32	7.3 ± 2.5	5.9 ± 2.4
Winter 2015	113.0 ± 11.9	62.6 ± 3.5	35.5 ± 3.2	20.9 ± 1.2	27.1 ± 0.9	1.9	0.57	0.59	0.34	11 ± 1.9	3.9 ± 0.3

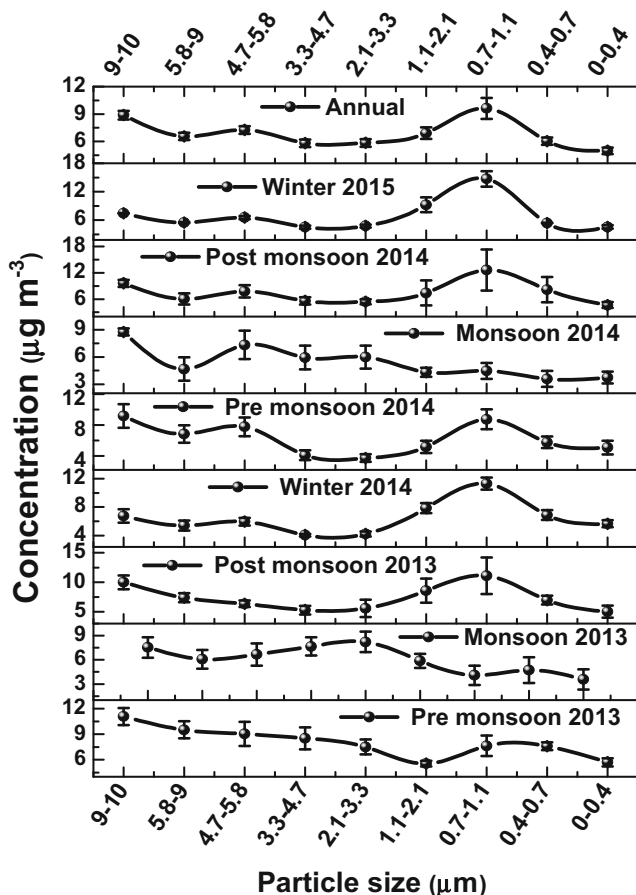


Fig. 3 Seasonal distributions of PM mass concentrations for nine size bins as classified by a cascade impactor

Kopanakis et al. (2012) at an urban site in Greece with fine (coarse) mode particle concentration dominance at an aerodynamic diameter of less than 1 µm (between 3.3 and 9 µm). Also, Temesi et al. (2001) noticed similar distribution at a rural site in Hungary with a 13-stage low-pressure impactor, whereas

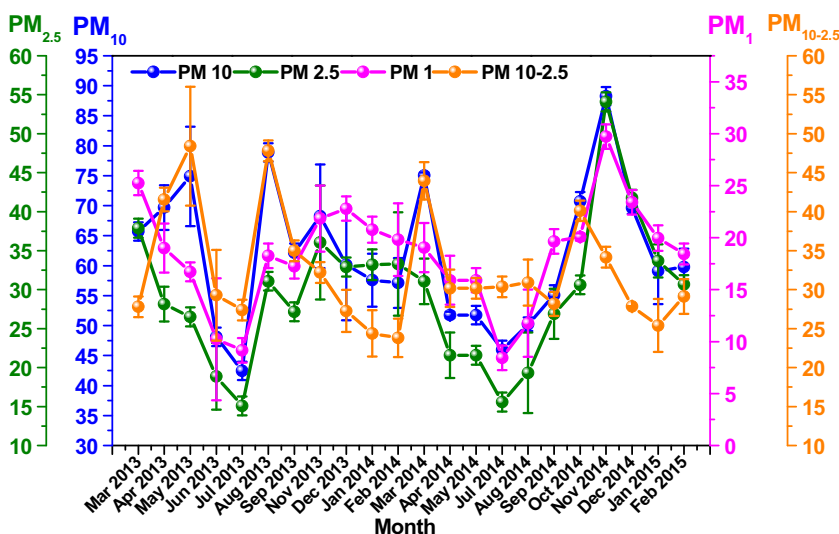
Neusüss et al. (2000) observed a monomodal distribution in Leipzig (Germany) by using a five-stage Berner impactor.

Monthly and seasonal variations of PM

In order to understand the percentage contributions of PM_{10-2.5} (coarse), PM_{2.5} (fine) and PM₁ (ultrafine) in total PM, we have accounted their mass concentrations separately and studied monthly (see Fig. 4) as well as seasonal variations (see Table 1) measured during the studied period. The average mass concentration of PM_{2.5} (PM₁) for the studied period was observed as follows: post-monsoon 34.4 ± 2.8 µg m⁻³ (21.3 ± 2.0 µg m⁻³), winter 34.3 ± 1.17 µg m⁻³ (21.1 ± 0.3 µg m⁻³), pre-monsoon 27.8 ± 3.0 µg m⁻³ (18.6 ± 1.7 µg m⁻³) and monsoon 19.5 ± 2.1 µg m⁻³ (11.3 ± 1.2 µg m⁻³). However, in the case of PM_{10-2.5}, it was found to be in the following decreasing order as pre-monsoon (37.0 ± 2.25 µg m⁻³), post-monsoon (33.9 ± 0.3 µg m⁻³), monsoon (32.7 ± 2.1 µg m⁻³) and winter (26.2 ± 1 µg m⁻³). Consequently, PM₁₀ concentrations were notably higher during post-monsoon (68.3 ± 3.0 µg m⁻³) and pre-monsoon (64.8 ± 5.3 µg m⁻³) seasons followed by the winter (60.5 ± 2.2 µg m⁻³), with a lower value during the monsoon (52.3 ± 4.2 µg m⁻³) season.

For PM_{2.5} (PM₁), the concentrations were higher during post-monsoon and winter seasons which are due to persistent thermal inversion and foggy conditions at ground level causing an increase in the aerosol concentration near the surface. Aerosol hygroscopic nature due to the availability of high relative humidity may enhance the particle concentration, and also, long-range transport of pollutants from the heavily polluted regions elevated the particle concentration for PM₁₀ during the post-monsoon season. Similar results but with high magnitudes were reported by Tiwari et al. (2009, 2013) over the

Fig. 4 Monthly variations of different PM fractions PM₁₀, PM_{10-2.5}, PM_{2.5} and PM₁ over Kadapa. The corresponding mean seasonal values are presented in Table 1



national capital region Delhi in India. In case of the coarse particle ($PM_{10-2.5}$), higher concentrations were observed during the pre-monsoon season which is attributed to the strong winds. Also, the prevailing high local temperatures make soil loose that resulted in uplift of soil dust particles that favoured re-suspension and transport of dust (coarse mode) particles towards the measurement site (Balakrishnaiah et al. 2011). The similar results which are in good agreement with the present findings have been reported by Balakrishnaiah et al. (2011), Spindler et al. (2010), Qiu and Pattey (2008) and so on. The low levels of PM fractions over the study region usually recorded during the monsoon season which could be evident from the rain or washout processes (see Fig. 2a) and also the long-range transport of advected air masses from the marine environment, which will be discussed in the following sections.

From the polar contour maps shown in Fig. 5, the maximum PM_{10} concentration was noticed when the direction of the wind is from NE to N, east, west and SW directions. In the case of $PM_{10-2.5}$, the significant concentration was noticed at higher wind speeds (~ 4.0 –

4.5 m s^{-1}) in the NE and SW directions, followed by all the directions but with less wind speed ($< 3.5 \text{ m s}^{-1}$). Whereas, the maximum concentrations of $PM_{2.5}$ were observed from the SW to west and in the NE directions. The concentrations of PM were completely absent in the NW direction. In the case of PM_1 , the dominant concentrations but with smaller magnitude were observed in north, south and east directions. But significant concentrations of PM_1 were observed in all the direction except for the SW direction. Further, we also observed the distribution of PM mass concentrations for different size fraction drawn as a function of wind speed and direction (see Fig. S3 of SM). It is clear that the larger coarse particles having a mode in the range 4.7 – 6.8 , 6.8 – 9.0 and 9 – $10 \mu\text{m}$ were completely absent when the winds were in the NE direction. Similarly, small particle concentrations having modes in the range 0.4 – 0.7 , 0.7 – 1.1 and 1.1 – $2.1 \mu\text{m}$ were absent when the winds were originated from the SW direction towards the observational site.

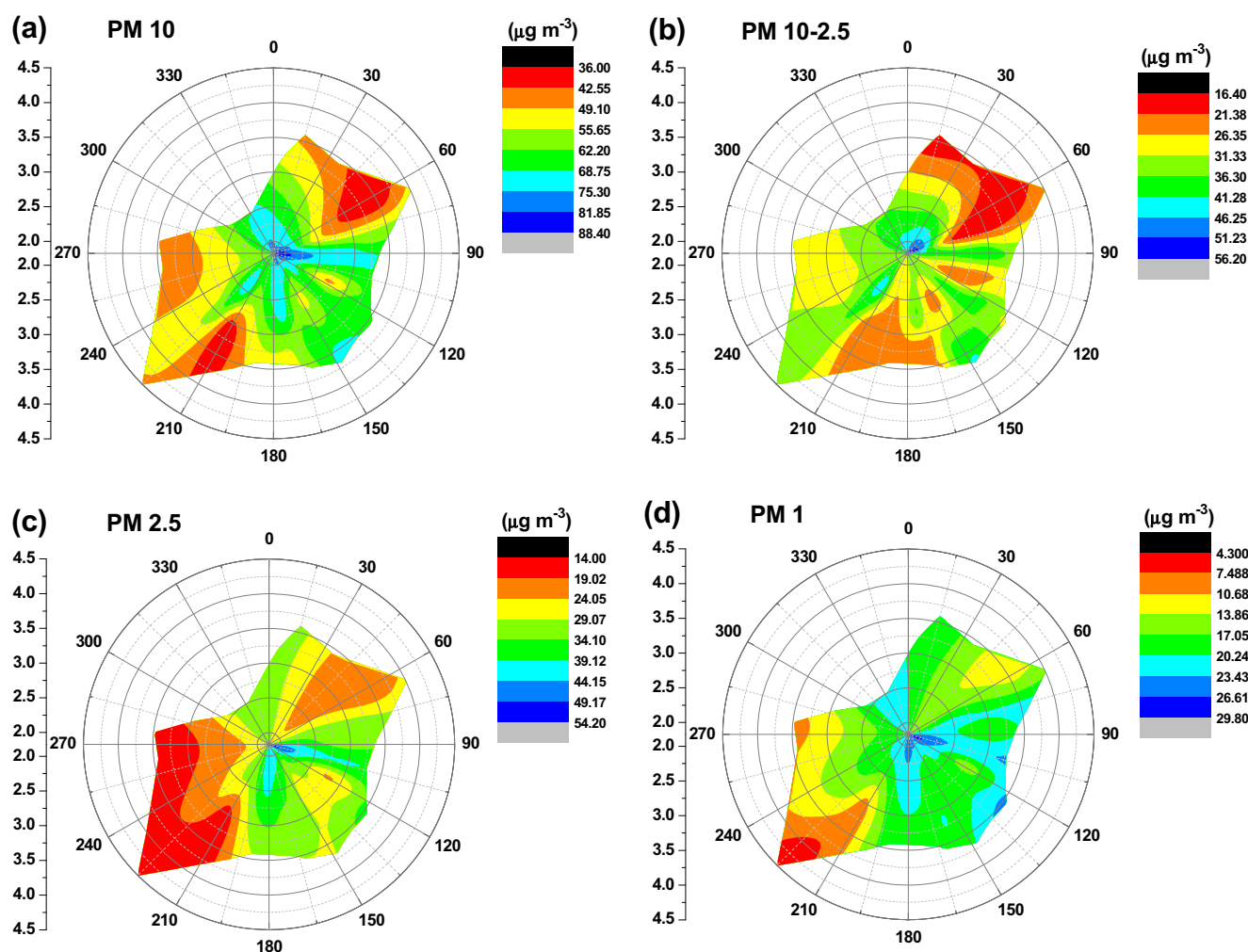


Fig. 5 Polar contour plots of different PM fractions **a** PM_{10} , **b** $PM_{10-2.5}$, **c** $PM_{2.5}$ and **d** PM_1 as a function of wind speed and wind direction over Kadapa

Seasonal variations in TSPM

The season-wise variations of TSPM concentrations observed at the measurement site were illustrated in Table 1. High TSPM concentrations were found during the winter ($93 \pm 11.1 \mu\text{g m}^{-3}$) followed by the pre-monsoon ($88 \pm 8.5 \mu\text{g m}^{-3}$) and post-monsoon seasons ($80 \pm 15.4 \mu\text{g m}^{-3}$), with low values of concentration in monsoon ($60 \pm 9.4 \mu\text{g m}^{-3}$). High TSPM during winter season may be attributed to local anthropogenic activities such as burning for domestic cooking purposes and surface heating, etc. In addition, the local meteorology also supports for the enhancement of particle concentrations due to the low and steady winds over the study region. Low TSPM concentration was found during the monsoon season which is due to frequent rains as the study region experiences during these seasons resulted in the washout of pollutant at the ground level.

The average mass concentration of TSPM in the present study was found to be $80 \pm 8 \mu\text{g m}^{-3}$, which is double than that observed over nearby (~ 120 km) semi-arid site, Anantapur ($34 \mu\text{g m}^{-3}$), as reported by Reddy et al. (2013) and also higher than the concentration reported over high altitude site, Manora peak (Ram et al. 2010a). Comparatively, low TSPM concentrations were observed at this location than the values reported over the Indo-Gangetic Plain (IGP) which is a heavily polluted region over North India (Ram and Sarin 2010 and references therein). Statistical analysis showed that PM_{10} was about 79 % of TSPM at Kadapa, which is a very high percentage value compared to the two different areas Kasba (a residential area) and Cossipore (an industrial area) with 52 and 54 % of TSPM, respectively, in Kolkata as investigated by Karar et al. (2006).

Further, the percentage of black carbon (BC) in TSPM was estimated and noticed an annual mean of 2.7 % at Kadapa during the study period. On a seasonal basis, these variations were observed to be high during the pre-monsoon (3.24 %) and winter (3.17 %) seasons followed by the post-monsoon (2.74 %) and low value observed during the monsoon season 1.93 % (see Table 1). The monthly variations of the percentage of BC in TSPM were found to be high in November 2013 (4.88 %) and low in the months of July 2013 and June 2014 (1.42 %). The percentage of BC in TSPM measured in the present study was found to be low when compared to another semi-arid region, Challakere (3.3 %) in Karnataka (India) as examined by Satheesh et al. (2013).

PM ratios and their relationship

The ratio between $\text{PM}_{2.5}$ and PM_{10} was calculated on a monthly basis at Kadapa and exhibited a large month-to-month variability, ranging from 0.34 (July 2014) to 0.61 (November 2014) with a mean value of 0.47 (see Table 1). This ratio is comparable with that of the value of 0.48 reported

by Fang and Chang (2010) over a rural site in Taiwan (Guanyin) and higher (~ 0.4) than the value observed by Alghamdi et al. (2014) for Saudi Arabia. However, the mean ratio between $\text{PM}_{10-2.5}$ and PM_{10} observed at the present studied region was 0.53, ranging from 0.39 (November 2014) to 0.66 (June 2014). Season-wise ratios between $\text{PM}_{2.5}$ and PM_{10} were also analysed at the sampling site and are presented in Table 1. The highest $\text{PM}_{2.5}/\text{PM}_{10}$ ratio was found during the winter (0.57) followed by the post-monsoon season (0.5) and low values during monsoon (0.37) and pre-monsoon (0.43) seasons.

This shows that the maximum contribution of fine particles ($\text{PM}_{2.5}$) was observed during winter and coarse ($\text{PM}_{10-2.5}$) particle contribution during the monsoon and pre-monsoon seasons, whereas both have equal contributions during the post-monsoon. Consequently, quite opposite correlation was found in the ratio of $\text{PM}_{10-2.5}/\text{PM}_{10}$ with an average value of 0.53. Residential heating during winter would be the main cause for the increases of $\text{PM}_{2.5}/\text{PM}_{10}$ ratio, while the strong winds in monsoon increase the concentration of coarse particles in the air, which decreases the ratios of $\text{PM}_{2.5}/\text{PM}_{10}$. Similarly, high and low ratios of $\text{PM}_{2.5}/\text{PM}_{10}$ that were observed during the winter and monsoon seasons, respectively, were reported by Singh et al. (2013) over an urban site, Delhi in India.

The annual mean seasonal ratios of $\text{PM}_1/\text{PM}_{2.5}$ ($\text{PM}_1/\text{PM}_{10}$) for the 2 years followed the decreasing order of 0.67 (0.35), 0.62 (0.31), 0.61 (0.29) and 0.58 (0.22) for pre-monsoon (winter), post-monsoon (post-monsoon), winter (pre-monsoon) and monsoon (monsoon) seasons, respectively. The $\text{PM}_{2.5}$ was mainly composed of PM_1 at a significant proportion of 62 % for the study period. The $\text{PM}_{2.5}/\text{PM}_{10}$ ratios reported in this study were lower, which endorse the interpretation that TSPM and PM_{10} were largely derived from arid lands surrounding the observational site. This was in contrast with the other sites where $\text{PM}_{2.5}$ was the major contributor to PM_{10} as well as TSPM (Tiwari et al. 2014; Deshmukh et al. 2013 and references therein).

Correlation analyses between different particulates have been studied over the observational site. The scatter plot drawn between TSPM and PM_{10} and TSPM and $\text{PM}_{10-2.5}$ showed positive correlations with coefficients (r) of 0.83 and 0.70, respectively. Also, the correlations of PM_{10} vs. $\text{PM}_{10-2.5}$ and PM_{10} vs. $\text{PM}_{2.5}$ found to be good with correlation coefficients of $r = 0.78$ and $r = 0.72$, respectively. Also, the strong positive correlation coefficient of $r = 0.90$ and a fair correlation coefficient of 0.64 have been observed for the scatters of $\text{PM}_{2.5}$ and PM_1 and PM_{10} and PM_1 , respectively (see Table S1 of SM).

The calculated annual mean percentage of BC mass fraction in $\text{PM}_{2.5}$ was 7.13 % during the study period at Kadapa. We found high values of 10.4 % during the pre-monsoon 2014 attributed to intense forest fires/burning over the Nallamala

forest (NE direction) which is in agreement with the results reported by Begam et al. (2016). The low value was observed during the post-monsoon 2014 due to lesser availability of BC data as measured by the instrument due to its operational failure during November 2014, and also, more precipitation from the NE monsoon washes out the aerosols (see Table 1).

Comparison of PM with other sites

We compared our results with the previous measurements reported by several authors in India and other sites in the world. The $PM_{2.5}$ concentration over the measurement site was in accordance with the results ($28.6 \pm 14.6 \mu\text{g m}^{-3}$) pointed out by Satsangi et al. (2011) for an urban site, Agra (India), and Fang and Chang (2010) for a rural site ($28 \mu\text{g m}^{-3}$) in Taiwan (Guanyin). We also compared the PM_{10} concentrations and were in good agreement with the values reported by Bell et al. (2006) examined over Mexico City ($60.2 \mu\text{g m}^{-3}$). The recorded values in the present study were slightly higher than the values investigated by Ahmed et al. (2015) ($PM_{2.5} 26.6 \pm 2.6 \mu\text{g m}^{-3}$; $PM_{10} 54.0 \pm 15.0 \mu\text{g m}^{-3}$) for an urban environment in Korea.

The results obtained in the present study showed that the PM concentrations were higher compared to the other sites reported in the literature. Mouli et al. (2006) explored lower PM_{10} ($32.7 \mu\text{g m}^{-3}$) at a suburban site, Tirupati in southern peninsular India. Also, the average values of PM_{10} ($18.7 \mu\text{g m}^{-3}$) and $PM_{2.5}$ ($17.1 \mu\text{g m}^{-3}$) given by Balakrishnaiah et al. (2011) for a semi-arid site Anantapur (India) were also lower than that of the values presented in our study. Similarly, Hieu and Lee (2010) reported $PM_{1.0}$ $18.5 \mu\text{g m}^{-3}$, $PM_{2.5}$ $27.6 \mu\text{g m}^{-3}$ and PM_{10} $50.5 \mu\text{g m}^{-3}$ for Korea, and Pateraki et al. (2010) showed PM_{10} , $PM_{2.5}$ and $PM_{2.5-10}$ 34.8, 18.0 and $23.8 \mu\text{g m}^{-3}$ for Europe. Further, Lazaridis et al. (2008) and Gugamsetty et al. (2012) observed the concentrations of 35.0 ± 17.7 and $25.4 \pm 16.5 \mu\text{g m}^{-3}$ and 39.45 ± 11.58 and $21.82 \pm 7.50 \mu\text{g m}^{-3}$ for PM_{10} and $PM_{2.5}$ at Greece and Shinjung (Taiwan).

Some previous studies, particularly over North India, depicted very high values of PM_{10} and $PM_{2.5}$ concentrations when compared with the present study. We illustrated this with the help of certain studies reported by Tiwari et al. 2014 (130 ± 103 and $222 \pm 142 \mu\text{g m}^{-3}$ for $PM_{2.5}$ and PM_{10}) over Delhi, Deshmukh et al. 2013 (PM_{10} , $PM_{2.5-10}$, $PM_{2.5}$ and PM_1 were of 270.5 ± 105.5 , 119.6 ± 44.6 , 150.9 ± 78.6 and $72.5 \pm 39.0 \mu\text{g m}^{-3}$, respectively) for Raipur, Das et al. (2006) (PM_{10} $304 \mu\text{g m}^{-3}$; $PM_{2.5}$ $179 \mu\text{g m}^{-3}$) for Kolkata and Sharma and Maloo (2005) (PM_{10} $272.0 \mu\text{g m}^{-3}$; $PM_{2.5}$ $146.0 \mu\text{g m}^{-3}$) over Kanpur. From all these studies, it is clear that the particle pollution has become a more serious threat in northern India when compared to southern India. This may be due to large heterogeneity in the emission of regional sources due to rapid industrialization/urbanization and also large

differences in meteorological conditions. For North Indian sites, the levels described by NAAQS of India were particularly high and always above these levels compared to south Indian regions, not only in the PM levels but also in the BC aerosol (Tiwari et al. 2014) which were higher than the southern Indian regions (e.g., Begam et al. 2016; Kumar et al. 2011 and references therein). Recently, there has been significant focus on studying aerosols over the IGP due to the presence of high pollutant concentrations and its effects on the regional climate (Singh et al. 2004; Ram et al. 2010a; Gautam et al. 2011; Lodhi et al. 2013; Tiwari et al. 2014).

WSIC in TSPM

The percentage contribution was calculated between each individual ion and ionic mass, followed by an order $SO_4^{2-} > NO_3^- \sim Cl^- > F^- \sim PO_4^{2-} > NO_2^-$ for anions and $Na^+ > Ca^{2+} > K^+ \sim NH_4^+ > Mg^{2+}$ for cations. The higher portion was occupied by SO_4^{2-} (28.99 %) to the WSIC mass followed by Na^+ (12.48 %) and Ca^{2+} (11.93 %). The contribution of cations share in WSIC was high (~44 %) over the observational site (Fig. 6a). Further, the seasonal mean mass concentrations of different ions in TSPM are shown in Table. 2.

The average concentration of SO_4^{2-} was $11.7 \mu\text{g m}^{-3}$ (28.99 % in WSIC, Fig. 6a). A possible reason could be due to mining activities (Barites mining) or aqueous-phase oxidation of SO_2 in cloud droplets (Seigneur and Saxena 1988). The present study region is far away from the coastal region; hence, sea salt contribution was insignificant. This was further confirmed by high SO_4^{2-}/Na^+ ratio (2.44). Similarly, high SO_4^{2-} ($5.72 \mu\text{g m}^{-3}$) concentration was reported by Mouli et al. (2006) at a suburban site, Tirupati, which is attributed to the soil-derived component or formed by reactions of gas-phase SO_2 on the wet surface of basic soil particles. Also, this may be due to the transport of pollutants originated from the IGP region towards the measurement site with the action of favourable winds during the post-monsoon and winter seasons (Rastogi et al. 2015). The average concentration of NO_3^- was $3.95 \mu\text{g m}^{-3}$ (9.75 %, Fig. 6a). The mass ratio of NO_3^-/SO_4^{2-} varied from 0.15 to 0.79, with an annual mean of 0.39. This is similar and agreement with that of the value of 0.44 reported by Gao et al. (2011) over Jinan (East China). The relatively low ratio of NO_3^-/SO_4^{2-} , i.e., less than 1.0 indicated that stationary sources like industrial emissions played more important role compared to mobile sources (Lai et al. 2007), like vehicular emissions over the study region Kadapa.

The average concentrations of Na^+ and Cl^- were found to be of $4.8 \mu\text{g m}^{-3}$ (12.48 % in WSIC) and $3.8 \mu\text{g m}^{-3}$ (9.54 % in WSIC), respectively. The ratio of Cl^-/Na^+ in aerosols (0.8) was less than the seawater ratio, i.e., 1.79 (Möller 1990), indicating a lack of chloride concentration with respect to Na^+ concentration. As we have already mentioned that our observational site is far from the sea coast (~300 km), hence, loss of Cl^- in the PM may

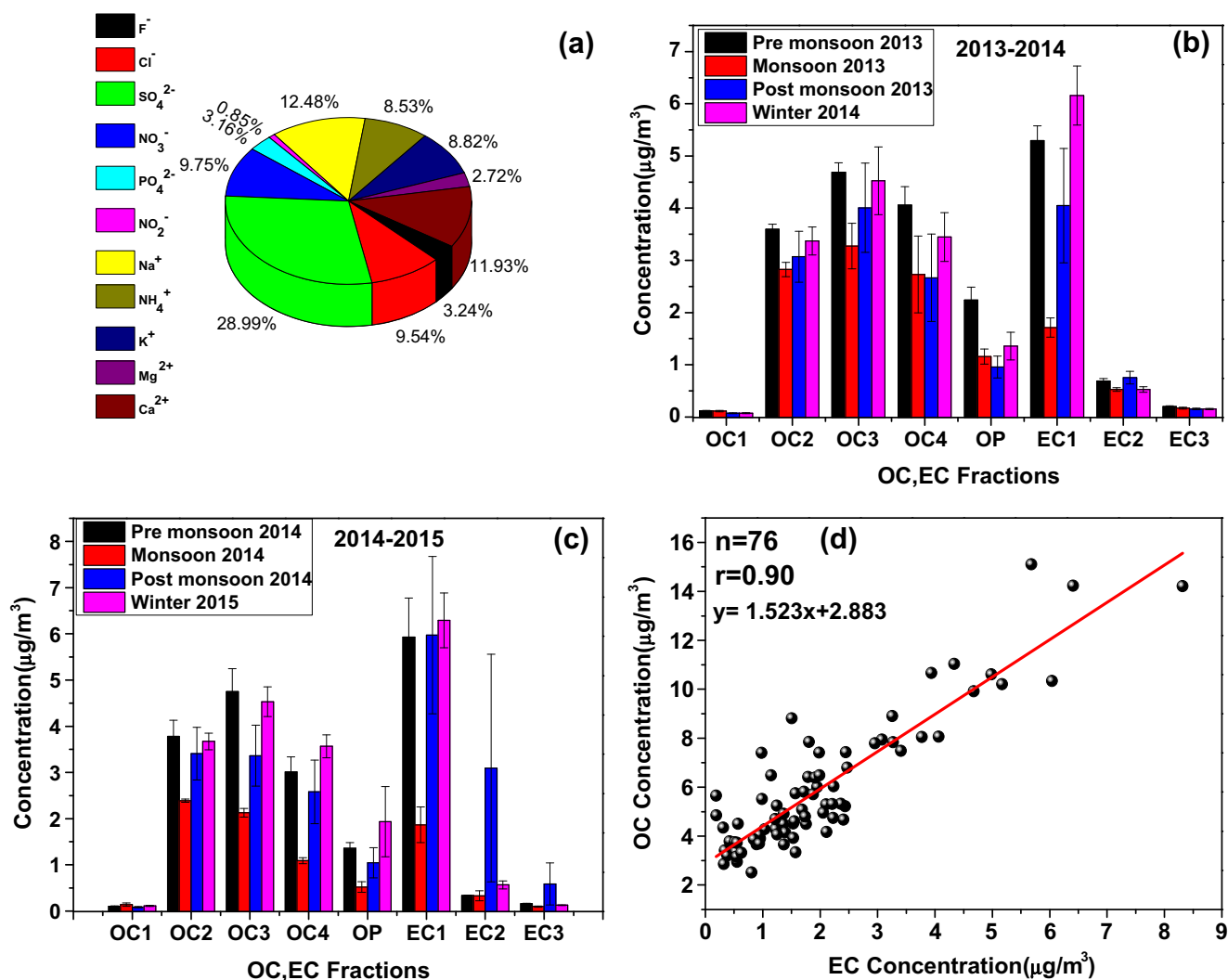


Fig. 6 a Average percentage contribution of different ionic components to the total WSIC. Seasonal analysis of OC and EC during the study

period b 2013–2014 and c 2014–2015. d Scatter plot between OC and EC for the study period at Kadapa

be a chemical reaction between H₂SO₄ and HNO₃ with NaCl to produce HCl (Mouli et al. 2003) and also dilution of Cl⁻.

The average concentration of K⁺ was only 3.4 μg m⁻³ (8.82 %, see Fig. 6a) in the total. The main source for the occurrence of K⁺, Ca²⁺ and Na⁺ over the site is mainly from the Granite mining activity (which contains 65 % alkaline feldspar with a mixture of Na⁺, K⁺, Ca²⁺ and 20 % of quartz) taking place in the NW direction to the observational site. Hence, these ions were present in the PM due to the continuous mining activity. The observed average concentration of NH₄⁺ was 7.3 μg m⁻³ (8.53 % in WSIC) over the observational site which is from the agricultural farmlands and anthropogenic activities around the observational site.

Fractions of carbonaceous aerosols (OC and EC) in TSPM

The OC and EC fractions of carbonaceous aerosols in TSPM are given in Fig. 6b, c for different seasons during the study

period. The high concentrations of OC2, OC3, OC4 and OP were observed during the pre-monsoon followed by the winter season which is attributed from the coal combustion for domestic activities, motor vehicular exhaust and biomass burning from the surrounding agricultural fields. The high concentrations of EC2 and EC3 were due to the diesel vehicle exhaust, as it is the mixture of a lot of high-temperature components of EC particles (Watson et al. 1994). From Fig. 6b, the high EC2 and EC3 concentrations were noted during the post-monsoon season followed by the pre-monsoon. The difference in concentration of OC1 is negligible, and this may be due to the presence of common significant source such as biomass burning irrespective of the seasons.

During winter 2015, notably high concentration was observed for OC (11 ± 1.9 μg m⁻³) followed by the post-monsoon 2014 (7.2 ± 2.5 μg m⁻³), whereas EC maximum concentration was found during the post-monsoon 2014 (5.8 ± 2.3 μg m⁻³) followed by the winter 2015

Table 2 The mean mass concentration of WSIC in TSPM during the measurement period at Kadapa

Season	F ⁻ ($\mu\text{g m}^{-3}$)	Cl ⁻ ($\mu\text{g m}^{-3}$)	SO ₄ ²⁻ ($\mu\text{g m}^{-3}$)	NO ₃ ⁻ ($\mu\text{g m}^{-3}$)	PO ₄ ²⁻ ($\mu\text{g m}^{-3}$)	NO ₂ ⁻ ($\mu\text{g m}^{-3}$)	Na ⁺ ($\mu\text{g m}^{-3}$)	NH ₄ ⁺ ($\mu\text{g m}^{-3}$)	K ⁺ ($\mu\text{g m}^{-3}$)	Mg ²⁺ ($\mu\text{g m}^{-3}$)	Ca ²⁺ ($\mu\text{g m}^{-3}$)
Monsoon 2013	2.88	6.67	7.10	3.15	1.03	-	6.43	-	2.38	1.06	7.49
Post-monsoon 2013	1.72	3.78	11.29	3.68	1.00	2.46	8.59	-	10.40	1.00	3.88
Winter 2014	0.82	1.35	13.32	3.41	2.22	-	3.43	0.23	1.07	0.85	2.59
Pre-monsoon 2014	0.24	1.76	12.08	5.08	2.42	1.16	5.10	3.05	1.66	0.86	2.44
Monsoon 2014	0.08	4.28	13.96	5.36	3.74	-	5.25	0.46	1.94	1.12	1.56
Post-monsoon 2014	2.36	8.86	3.99	2.18	3.21	0.88	2.99	15.93	2.76	0.97	1.75
Winter 2015	0.56	1.40	17.94	3.87	-	-	2.90	10.64	4.98	1.22	10.80

($3.9 \pm 0.2 \mu\text{g m}^{-3}$) season (Fig. 6c). Furthermore, the total carbon (TC) was noted high during winter 2015 ($15 \pm 1.6 \mu\text{g m}^{-3}$), followed by the post-monsoon ($13.1 \pm 4.1 \mu\text{g m}^{-3}$). Similarly, the respective low concentrations of 3.9 ± 0.1 , 0.6 ± 0.1 and $4.9 \pm 0.3 \mu\text{g m}^{-3}$ were observed for OC, EC and TC during the monsoon seasons of 2013 and 2014. It is evident that the annual average concentrations of OC, EC and TC during the study period at Kadapa were found to be 6.2 ± 0.7 , 2.5 ± 0.6 and $8.8 \pm 1.2 \mu\text{g m}^{-3}$, respectively.

High OC and EC concentrations were found during the winter ($8.4 \pm 1.6 \mu\text{g m}^{-3}$) and post-monsoon ($4.0 \pm 2.1 \mu\text{g m}^{-3}$), respectively, for the study period at the sampling site. High OC and EC concentrations during the winter and post-monsoon seasons (see Table 1) may be attributed from agricultural biomass burning to clear the harvest in the farmlands, wood and garbage burning. Further, the long-range transport of pollutants from the IGP region also played important role in bringing the carbonaceous particles for the study region Kadapa. Due to low wind speed, the pollutants emitted from the local anthropogenic activities like field crops cultivation may induce a large amount of OC particles into the air during winter.

Figure 6d shows the scatter plot between OC and EC with a significantly strong correlation coefficient of $r = 0.9$ (with a slope of 1.52), indicating similar sources for the occurrence of OC and EC over the study region (Salma et al. 2004). The seasonal average OC/EC ratio was varied between 2.1 and 9.4, with an annual average of 4.2 during the study period at Kadapa. This ratio is well comparable with the value reported by Sharma et al. (2014) for an urban site, Delhi in India, and Paraskevopoulou et al. (2015) for the suburban region in Athens (Greece). If the OC/EC ratio value exceeds the cut-off point of 2.0, it confirms the existing of secondary organic aerosols (Chow et al. 2001). In the present study, the OC/EC is 4.2 that indicates the formation of secondary organic aerosol over the semi-arid rural region Kadapa. Ram et al. (2010a, b) pointed out that higher OC/EC ratio was attributed to more biomass burning and lower ratios are due to the frequent fossil fuel burnings. Further, a recent study by Li et al. (2016) reported low OC/EC values (3.07 ± 0.86 and 2.94 ± 1.19) for the study regions (Xianlin and Gulou) in Nanjing, China.

Role of long-range air mass transport

The 5-day back trajectory analysis obtained at an elevation of 500 m above sea level was performed by using the Hybrid Single Particle Lagrangian Integrated Trajectory (HYSPPLIT) model (<http://www.arl.noaa.gov/ready/hysplit4.html>) (Draxler and Rolph 2003) over the observational site, which gives good insight into the origin and transport of air parcels arriving at the sampling site. The long-range transport of aerosols during the pre-monsoon season showed different advection pathways forming different clusters originating from

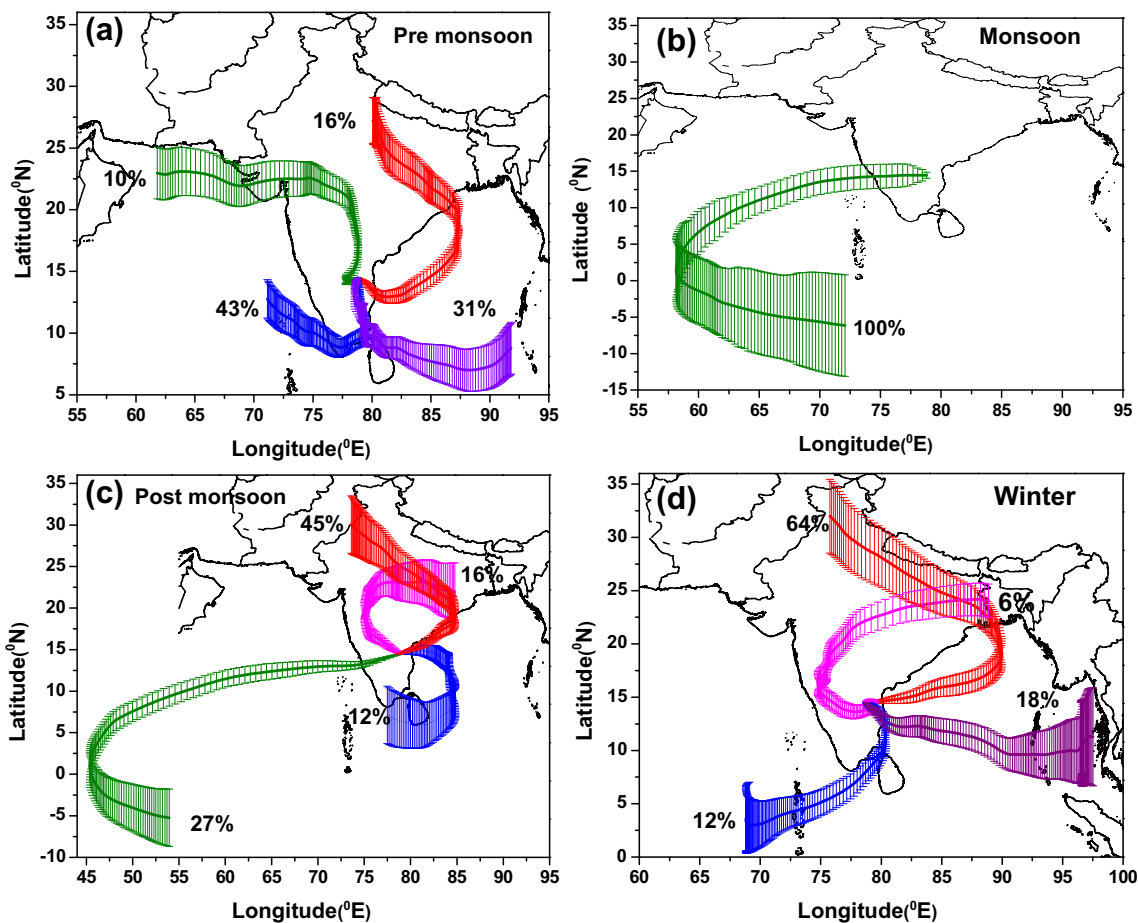


Fig. 7 HYSPLIT cluster trajectory analysis derived at 500 m above sea level for different seasons during the study period over Kadapa

different locations (Fig. 7a). Among these cluster groups of trajectories, maximum percentages of (74 %) trajectories were originated from the marine environment (the Bay of Bengal (BoB) and the Arabian Sea (AS)) and reached to the observational site by traversing through the south Indian urban/industrial and coastal regions resulted in transport of polluted air mass. The remaining 16 % of trajectories were coming from IGP region which is heavily polluted and 10 % from the Indian west coast.

During the monsoon season (Fig. 7b), all the trajectories (100 %) were coming from the AS which is a characteristic feature of the study region as reported by several authors (e.g., Kumar et al. 2011; Tiwari et al. 2014; Begam et al. 2016 and references therein). The long-range transport of aerosol during the post-monsoon season showed maximum trajectories having continental overpass from the IGP region (61 %) passing through central India before reaching the sampling site. Apart from this, some trajectory groups (27 %) were transported from the oceanic regions of the AS, and the remaining trajectories (12 %) were covered the Indian Ocean, the BoB and the inland region of Sri Lanka.

During winter, most of the trajectories (64 %) were originated from the IGP region and diverted towards the BoB

before reaching the site. Whereas, 6 % of trajectory clusters were originated from the northeast Indian region covering the central Indian regions and finally arriving at the study region. The other 18 % of trajectory clusters were transported from the island regions of Thailand and Andaman and Nicobar Island. The remaining 12 % of trajectories originated from the AS and traversing through southeast Indian coastal regions before reaching the observational site. Therefore, the variability in the accumulation of air parcels before reaching the site was more predominant during during the wet seasons (from September 2014 to February 2015) resulted in increased aerosol loading.

Conclusions

The main conclusions drawn from the present study are summarized as follows:

1. The fine mode particle concentrations ($PM_{2.5}$, PM_{1}) were more dominant during the post-monsoon and winter seasons at Kadapa. This may be due to thermal inversion and foggy conditions at ground level, whereas coarse mode

particle concentrations were higher during the pre-monsoon season attributed to resuspension of soil-derived dust.

- The observed increase of $PM_{2.5}/PM_{10}$ (PM_1/PM_{10}) ratio during the winter is due to local residential heating for cooking purpose and biomass burning to get warmth against the cold winters, while the strong winds in monsoon increased the concentration of coarse particles in the air, which decreases the ratios of $PM_{2.5}/PM_{10}$ (PM_1/PM_{10}).
- During winter, fine particle ($PM_{2.5}$) contribution to the PM_{10} was higher and coarse ($PM_{10-2.5}$) particle contribution was dominated during the monsoon and pre-monsoon seasons, whereas both have equal contribution during the post-monsoon seasons.
- The mass ratio of NO_3^-/SO_4^{2-} ranged from 0.15 to 0.79, with an annual mean of 0.39. The relatively low mass ratio of NO_3^-/SO_4^{2-} indicates that stationary sources played more important role compared to mobile point sources.
- In the present study, it is evident from the ratio of OC/EC (which is 4.2) that the studied region is more dominated by the formation of secondary organic aerosols.
- HYSPLIT cluster trajectories revealed that the coarse mode particle contribution was mainly dominated during the pre-monsoon and monsoon seasons with air mass coming from the oceanic regions (BoB and AS), while the abundance in fine mode particle concentration was due to the long-range transport of air masses from the Indian mainland, particularly from the IGP region.

Acknowledgments The authors are indebted to Indian Space Research Organization (ISRO), Bangalore, for the financial support through its Geosphere-Biosphere Programme (GBP) under Aerosol Radiative Forcing over India (ARFI) project. One of the authors (G. Reshma Begam) acknowledges the Department of Science and Technology (DST), New Delhi, for awarding fellowship under INSPIRE Programme. We are particularly grateful to Dr. K. Krishna Moorthy, ISRO Head Quarters, Bangalore, and Dr. S. Suresh Babu, ARFI Project Director, Trivandrum, for their constant encouragement and support. We also thank the NOAA Air Resources Laboratory for providing the HYSPLIT transport dispersion model used in this study. The authors would like to acknowledge Prof. Gerhard Lammel, Editor-in-Chief of the journal, and the anonymous reviewers for their helpful comments and constructive suggestions towards the improvement of an earlier version of the manuscript.

References

- Ahmed E, Kim KH, Shon ZH, Song SK (2015) Long-term trend of airborne particulate matter in Seoul, Korea from 2004 to 2013. *Atmos Environ* 101:125–133
- Alghamdi MA, Shamy M, Redal MA, Khoder MI, Abdel Hameed AA, Elserougy S (2014) Microorganisms associated particulate matter: a preliminary study. *Sci Total Environ* 479–480:109–116
- Almeida SM, Pio CA, Freitas MC, Reis MA, Trancoso MA (2006) Source apportionment of atmospheric urban aerosol based on weekdays/weekend variability: evaluation of road re-suspended dust contribution. *Atmos Environ* 40:2058–2067
- Balakrishnaiah G, Kumar KR, Reddy BSK, Gopal KR, Reddy RR, Reddy LSS, Narasimhulu K (2011) Characterization of PM, PM10 and PM2.5 mass concentrations at a tropical semi-arid stations in Anantapur, India. *Ind J Radio Space Phys* 40:95–104
- Begam GR, Vachaspati CV, Ahammed YN, Kumar KR, Babu SS, Reddy RR (2016) Measurement and analysis of black carbon aerosols over a tropical semi-arid station in Kadapa, India. *Atmos Res* 171:77–91
- Bell ML, Davis DL, Gouveia N, Borja-Aburto VH, Cifuentes L (2006) The avoidable health effects of air pollution in three Latin American cities: Santiago, São Paulo, and Mexico City. *Environ Res* 100:431–440
- Cao JJ, Lee SC, Ho KF, Zhang XY, Zou SC, Fung K, Chow JC, Watson JG (2003) Characteristics of carbonaceous aerosol in Pearl River Delta region, China during 2001 winter period. *Atmos Environ* 37: 1451–1460
- Cheung HC, Chou CCK, Huang WR, Tsai CY (2013) Characterization of ultrafine particle number concentration and new particle formation in an urban environment of Taipei, Taiwan. *Atmos Chem Phys* 13: 8935–8946
- Chow JC, Watson JG, Crow D, Lowenthal DH, Merrifield T (2001) Comparison of IMPROVE and NIOSH carbon measurements. *Aerosol Sci Technol* 34:23–34
- Contini D, Cesari D, Genga A, Siciliano M, Ielpo P, Guascito MR, Conte M (2014) Source apportionment of size-segregated atmospheric particles based on the major water-soluble components in Lecce (Italy). *Sci Total Environ* 472:248–261
- Dan M, Zhuang G, Li X, Tao H, Zhuang Y (2004) The characteristics of carbonaceous species and their sources in PM2.5 in Beijing. *Atmos Environ* 38:3443–3452
- Das M, Maiti SK, Mukhopadhyay U (2006) Distribution of $PM_{2.5}$ and $PM_{10-2.5}$ in PM_{10} fraction in ambient air due to vehicular pollution in Kolkata megacity. *Environ Monit Assess* 122:111–123
- Deshmukh DK, Deb MK, Mkoma SL (2013) Size distribution and seasonal variation of size-segregated particulate matter in the ambient air of Raipur city, India. *Air Qual Atmos Health* 6:259–276
- Fang GC, Chang SC (2010) Atmospheric particulate (PM_{10} and $PM_{2.5}$) mass concentration and seasonal variation study in the Taiwan area during 2000–2008. *Atmos Res* 98:368–377
- Draxler, RR, Rolph, GD, (2003) HYSPLIT (HYbrid Single-Particle Langrangian Integrated Trajectory). Model access via NOAA ARL READY website NOAA Air Resources Laboratory, Silver Spring, MD (<http://www.arl.noaa.gov/ready/hysplit4.html>)
- Gao X, Yang L, Cheng S, Gao R, Zhou Y, Xue L (2011) Semi-continuous measurement of water-soluble ions in PM2.5 in Jinan, China: temporal variations and source apportionments. *Atmos Environ* 45: 6048–6056
- Gautam R, Hsu NC, Tsay SC, Lau KM, Holben B, Bell S (2011) Accumulation of aerosols over the indo-Gangetic plains and southern slopes of the Himalayas: distribution, properties and radiative effects during the 2009 pre-monsoon season. *Atmos Chem Phys* 11: 12841–12863
- Gerasopoulos E, Koulouri E, Kalivitis N, Kouvarakis G, Saarikoski S, M kel T, Hillamo R, Mihalopoulos N (2007) Size-segregated mass distributions of aerosols over eastern Mediterranean: seasonal variability and comparison with AERONET columnar size-distributions. *Atmos Chem Phys* 7:2551–2561
- Gugamsetty B, Wei H, Liu CN, Awasthi A, Hsu SC, Tsai CJ, Roam GD, Wu YC, Chen CF (2012) Source characterization and apportionment of PM_{10} , $PM_{2.5}$ and $PM_{0.1}$ by using positive matrix factorization. *Aerosol and Air Qual Res* 12:476–491

- Hieu NT, Lee BK (2010) Characteristics of particulate matter and metals in the ambient air from a residential area in the largest industrial city in Korea. *Atmos Res* 98:526–537
- Karar K, Gupta AK, Animesh Kumar Biswas AK (2006) Characterization and identification of the sources of chromium, zinc, lead, cadmium, nickel, manganese and iron in PM₁₀ particulates at the two sites of Kolkata, India. *Environ Monit Assess (Netherlands)* 120:347–360
- Kopanakis I, Eleftheriadis K, Mihalopoulos N, Lydakakis-Simantiris N, Katsivela E, Pentari D, Zampas P, Lazaridis M (2012) Physico-chemical characteristics of particulate matter in the eastern Mediterranean. *Atmos Res* 106:93–107
- Kumar KR, Narasimhulu K, Balakrishnaiah G, Reddy BSK, Gopal KR, Reddy RR, Satheesh SK, Moorthy KK, Babu SS (2011) Characterization of aerosol black carbon over a tropical semi-arid region of Anantapur, India. *Atmos Res* 100:12–27
- Lai SC, Zou SC, Cao JJ, Lee SC, Ho KF (2007) Characterizing ionic species in PM_{2.5} and PM₁₀ in four Pearl River Delta cities. *South China J Environ Sci* 19:939–947
- Lazaridis M, Dzumbova L, Kopanakis I, Ondracek J, Glytsos T, Aleksandropoulou V, Voulgarakis A, Katsivela E, Mihalopoulos N, Eleftheriadis K (2008) PM₁₀ and PM_{2.5} levels in the eastern Mediterranean (Akrotiri Research Station, Crete, Greece). *Water Air Soil Pollut* 189:85–101
- Li HM, Wang QG, Yang M, Li FY, Wang JH, Sun YX, Wang C, Wu H, Qian X (2016) Chemical characterization and source apportionment of PM_{2.5} aerosols in a megacity of Southeast China. *Atmos Res* 181:288–299
- Lodhi NK, Beegum SN, Singh S, Kumar K (2013) Aerosol climatology at Delhi in the western indo-Gangetic plain: microphysics, long-term trends, and source strengths. *J Geophys Res* 118:1361–75–3276
- Möller D (1990) The Na/Cl ration in rainwater and the sea salt chloride cycle. *Tellus* 42(3):254–262
- Mouli PC, Venkata Mohan S, Jayarama Reddy S (2003) A study on major inorganic ion composition of atmospheric aerosols at Tirupati. *J Haz Mat B* 96:217–228
- Mouli PC, Venkata Mohan S, Jayarama Reddy S (2006) Chemical composition of atmospheric aerosol (PM₁₀) at a semi-arid urban site: influence of terrestrial sources. *Environ Monit Assess* 117:291–305
- Na K, Sawant AA, Song D, Cocker DR III (2004) Primary and secondary carbonaceous species in the atmosphere of western Riverside County, California. *Atmos Environ* 38:1345–1355
- Navrátil T, Hladil J, Strnad L, Koptíková L, Skála R (2013) Volcanic ash particulate matter from the 2010 Eyjafjallajökull eruption in dust deposition at Prague, Central Europe. *Aeolian Res* 9:191–202
- Neusüss C, Pelzing M, Plewka A, Herrmann H (2000) A new analytical approach for size-resolved speciation of organic compounds in atmospheric aerosol particles: methods and first results. *J Geophys Res* 105:4513–4527
- O'Brien DM, Mitchel RM (2003) Atmospheric heating due to carbonaceous aerosol in northern Australia—confidence limits based on TOMS aerosol index and sun-photometer data. *Atmos Res* 66:21–41
- Paraskevopoulou D, Liakakou E, Gerasopoulos E, Mihalopoulos N (2015) Sources of atmospheric aerosol from long-term measurements (5 years) of chemical composition in Athens, Greece. *Sci Total Environ* 527–528:165–178
- Pateraki S, Asimakopoulos DN, Maggos T, Vasilakos C (2010) Particulate matter levels in a suburban Mediterranean area: analysis of a 53-month long experimental campaign. *J Hazard Mater* 182: 801–811
- Pillai PS, Moorthy KK (2001) Aerosol mass-size distributions at a tropical coastal environment: response to mesoscale and synoptic processes. *Atmos Environ* 35:4099–4112
- Qiu G, Patteny E (2008) Estimating PM₁₀ emissions from spring wheat harvest using an atmospheric tracer technique. *Atmos Environ* 42: 8315–8321
- Ram K, Sarin MM (2010) Spatio-temporal variability in atmospheric abundances of EC, OC and WSOC over northern India. *J Aerosol Science* 41:88–98
- Ram K, Sarin MM, Tripathi SN (2010a) One-year record of carbonaceous aerosols from an urban location (Kanpur) in the indo-Gangetic plain: characterization, sources and temporal variability. *J Geophys Res*. doi:10.1029/2010JD014188
- Ram K, Sarin MM, Hegde P (2010b) Long-term record of aerosol optical properties and chemical composition from a high-altitude site (Manora peak) in central Himalaya. *Atmos Chem Phys* 10(23): 11791–11803
- Ramanathan V, Crutzen PJ, Kiehl JT, Rosenfeld D (2001) Aerosols, climate, and the hydrologic cycle. *Science* 294:2119–2124
- Rastogi N, Singh A, Sarin MM, Singh D (2015) Temporal variability of primary and secondary aerosols over northern India: impact of biomass burning emissions. *Atmos Environ*:1–8
- Reddy BSK, Kumar KR, Balakrishnaiah G, Gopal KR, Reddy RR, Sivakumar V, Arafath SM, Lingaswamy AP, Pavanakumari S, Umadevi K, Ahammed YN (2013) Ground-based in situ measurements of near-surface aerosol mass concentration over Anantapur: heterogeneity in source impacts. *Adv Atmos Sci* 30:235–246
- Rodriguez S, Querol X, Alastuey A, De la Rosa J (2007a) Atmospheric particulate matter and air quality in the Mediterranean: a review. *Environ Chem Lett* 5:1–7
- Rodriguez S, Dingenen RV, Putaud JP, Dell'Acqua A, Pey J, Querol X, Alastuey A, Chenery S, Ho KF, Harrison R, Tardivo R, Scamato B, Gemelli V (2007b) A study on the relationship between mass concentrations, chemistry and number size distribution of urban fine aerosols in Milan, Barcelona and London. *Atmos Chem Phys* 7: 2217–2232
- Salma I, Chi XG, Maenhaut W (2004) Elemental and organic carbon in urban canyon and background environments in Budapest, Hungary. *Atmos Environ* 38:2517–2528
- Satheesh SK, Krishna Moorthy K, Suresh Babu S, Srinivasan J (2013) Unusual aerosol characteristics at Challakere in Karnataka. *Current Sci* 104:5–10
- Satsangi PG, Kulshrestha Taneja A, Rao PSP (2011) Measurements of PM₁₀ and PM_{2.5} aerosols in Agra, a semi-arid region of India. *Indian J Radio Space Phys* 40:203–210
- Seigneur C, Saxena P (1988) A theoretical investigation of sulfate formation in clouds. *Atmos Environ* 22:105–115
- Seinfeld J Pandis S (1998) Air pollution to climate change. *Atmos Chem Phys*, Wiley
- Sharma M, Maloo S (2005) Assessment of ambient air PM₁₀ and PM_{2.5} and characterization of PM₁₀ in the city of Kanpur, India. *Atmos Environ* 39:6015–6026
- Sharma SK, Saxena M, Saud T, Korpole S, Mandal TK (2012b) Measurement of NH₃, NO, NO₂ and related particulates at urban sites of indo Gangetic plain (IGP) of India. *J Sci Indust Res* 71(5): 360–362
- Sharma SK, Mandal TK, Mohit Saxena Rashmi Sharma A, Datta A, Saud T (2014) Variation of OC, EC, WSIC and trace metals of PM₁₀ in Delhi, India. *J Atmos Sol Terr phys* 113:10–22
- Singh RP, Dey S, Tripathi SN, Tare V, Holben B (2004) Variability of aerosol parameters over Kanpur, northern India. *J Geophys Res* 109: D23206. doi:10.1029/2004JD004966
- Singh K, Tiwari S, Jha AK, Aggarwal SG, Bisht DS, Murty BP, Khan ZH, Gupta PK (2013) Mass-size distribution of PM₁₀ and its characterization of ionic species in fine (PM_{2.5}) and coarse (PM_{10-2.5}) mode, New Delhi, India. *Nat Hazards*. doi:10.1007/s11069-013-0652-8
- Spindler G, Bruggemann E, Gnauk T, Gruner A, Muller K, Herrmann H (2010) A four-year size-segregated characterization study of particles PM₁₀, PM_{2.5} and PM₁ depending on air mass origin at Melpitz. *Atmos Environ* 44:164–173

- Temesi D, Molnar A, Meszaros E, Feczko T, Gelencser A, Kiss G, Krivacsy Z (2001) Size resolved chemical mass balance of aerosol particles over rural Hungary. *Atmos Environ* 35:4347–4355
- Tiwari S, Srivastava AK, Bisht DS, Bano T, Singh S, Behura S, Srivastava MK, Chate DM, Padmanabhamurty B (2009) Black carbon and chemical characteristics of PM10 and PM2.5 at an urban site of North India. *J Atmos Chem* 62: 193–209. doi:10.1007/s10874-010-9148-z
- Tiwari S, Srivastava AK, Bisht DS, Parmita P, Srivastava MK, Attri SD (2013) Diurnal and seasonal variations of black carbon and PM2.5 over New Delhi, India: influence of meteorology. *Atmos Res* 125–126:50–62
- Tiwari S, Bisht DS, Srivastava AK, Pipal AS, Taneja A, Srivastava MK, Attri SD (2014) Variability in atmospheric particulates and meteorological effects on their mass concentrations over Delhi, India. *Atmos Res* 145–146:45–56
- Watson JG, Chow JC, Lowenthal DH, Pritchett LC, Frazier CA, Neuroth GR, Robbins R (1994) Differences in the carbon composition of source profiles for diesel-and gasoline-powered vehicles. *Atmos Environ* 28:2493–2505
- World Health Organization Europe (2005) Particulate matter air pollution: how it harms health. pp 1–4
- Xiang P, Zhou X, Duan J, Tan J, He K, Yuan C, Ma Y, Zhang Y (2017) Chemical characteristics of water-soluble organic compounds (WSOC) in PM2.5 in Beijing, China: 2011–2012. *Atmos Res* 183: 104–112